NREL
NATIONAL RENEWABLE ENERGY LABORATORY

# Thermal Performance of Uninsulated and Partially Filled Wall Cavities

## Preprint

El Hassan Ridouane and Marcus Bianchi

*Presented at the ASHRAE Annual Conference*
*Montreal, Quebec*
*June 25–29, 2011*



**Conference Paper**
NREL/CP-5500-50925
September 2011

Contract No. DE-AC36-08GO28308

**NOTICE**



Available electronically at http://www.osti.gov/bridge

Available for a processing fee to U.S. Department of Energy
and its contractors, in paper, from:

U.S. Department of Energy
Office of Scientific and Technical Information

P.O. Box 62
Oak Ridge, TN 37831-0062
phone: 865.576.8401
fax: 865.576.5728
email: mailto:reports@adonis.osti.gov

Available for sale to the public, in paper, from:

U.S. Department of Commerce
National Technical Information Service
5285 Port Royal Road
Springfield, VA 22161
phone: 800.553.6847
fax: 703.605.6900
email: orders@ntis.fedworld.gov
online ordering: http://www.ntis.gov/help/ordermethods.aspx

Cover Photos: (left to right) PIX 16416, PIX 17423, PIX 16560, PIX 17613, PIX 17436, PIX 17721

Printed on paper containing at least 50% wastepaper, including 10% post consumer waste.

# Thermal Performance of Uninsulated and Partially Filled Wall Cavities

**El Hassan Ridouane, PhD**
*Member ASHRAE*

**Marcus V. A. Bianchi, PhD**
*Member ASHRAE*

## ABSTRACT

*Low-rise, wood-framed homes are the most common type of residential structures in the United States. Wood wall construction supports roofs efficiently and provides a stable frame for attaching interior and exterior wall coverings. Wall cavities are prevalent and increase thermal resistance, particularly when they are filled with insulating material. This paper describes detailed computational fluid dynamics modeling to evaluate the thermal performance of uninsulated or partially filled wall cavities and accounts for conduction through framing, convection, and radiation. Parameters are ambient outdoor temperature, cavity surface emissivity, cavity aspect ratio, and insulation height. Understanding the thermal performance of uninsulated or partially insulated wall cavities is essential for conserving energy in residential buildings. The results can serve as input for building energy simulation tools such as DOE2 and EnergyPlus for modeling the temperature dependent energy performance of new and older homes with uninsulated or partially insulated walls.*

## INTRODUCTION

The study of heat transfer and fluid flow inside cavities of various shapes is an attractive area for fundamental and applied research. The pioneer studies were summarized by Jaluria (2003), Raithby and Hollands (1998), and Yang (1987). Numerous publications discuss natural convection flows in 2-D cavities of square and rectangular cross sections. Earlier work concentrated on pure natural convection with various thermal boundary conditions (Abourida et al. 1999, Douamna et al. 2000, Fusegi et al. 1992, and Lakhal et al. 1995), and on different aspect ratios and angles of inclination (Rahman and Sharif 2003). Experimental studies reported by Catton (1978) provided insight into the complexity of the problem. The interaction between natural convection and thermal radiation was the subject of numerical studies by Akiyama and Chong (1997), Pak and Park (1998), and Yucel et al. (1989). Their results showed that surface radiation significantly alters temperature distribution and flow patterns.

Barbour et al. (1994) focused on understanding the thermal behavior of steel-framed walls and reported that for metal stud walls with uninsulated cavities, the ASHRAE Zone Method overestimates thermal performance by up to 15%. Park et al. (1986) calculated heat transfer through the standard stud wall structure of a residential building. The wall cavities contained no insulation. They considered five test cases, with different approximations to the coupled heat transfer by convection and radiation. The assumption of constant temperature walls led to falsely high predictions for heat loss. This assumption does not reveal the substantial temperature differences between the top and bottom of the wall. The authors also found that thermal radiation is an important transport mechanism, even with modest temperature differences.

Lorente (2002) studied heat loss through building walls with closed, open, and deformable cavities, which appear in double-pane windows that have moderate pressure differences between the inner and outer panes. Heat losses are largely due to convective heat transfer inside vertical wall cavities. Air in wall structures is often falsely considered to be motionless. Aviram et al. (2001) used a guarded hot box to experimentally investigate the heat transfer through a variable aspect ratio cavity. Circulation intensity decreased and thermal resistance increased with increased aspect ratio. Similar numerical studies were conducted by Manz (2003) and Xaman et al. (2005) in rectangular cavities with aspect ratios 20, 40, and 80. Antar and Baig (2009) studied conjugate heat transfer by conduction and convection in a hollow block and showed that increasing the number of cavities while keeping the block width constant increased thermal resistance significantly. Vafai and Belwafa (1990) experimentally investigated heat transfer in cavities that were partially filled with fibrous insulation along the width.

**El Hassan Ridouane** is a Postdoctoral Researcher and **Marcus Bianchi** is a Senior Engineer, both in the Residential Building Systems Group at the National Renewable Energy Laboratory, Golden, CO.

They tested four samples with different densities and permeabilities in cavities of varying aspect ratios and concluded that reducing the insulation thickness (and thereby increasing the air gap thickness) increased heat transfer rates.

Despite the wealth of literature about vertical cavities, more information is needed for their application in whole-building energy simulation tools. Tools such as DOE2 and EnergyPlus use simplified, 1-D characterization that assumes a fixed thermal resistance over a building's temperature range. In reality, the thermal resistance of uninsulated and partially insulated cavities is affected by radiation and convection and is a function of several parameters, including temperature, surface emissivity, and aspect ratio. The objective of the present work is to fill this gap by performing direct numerical simulations of heat transfer by convection and radiation in air-filled and partially insulated wall cavities. These cavities, partially insulated along the height, appear in new and existing construction. In new construction, the walls may not be filled all the way, leaving a gap at the top of the cavity. In existing construction, the insulation material may settle. The outcomes of this study provide:

- Accurate input for whole-building simulations models such as DOE2 and EnergyPlus in different operating conditions
- Information necessary to provide recommendations for retrofit measures.

## NUMERICAL MODEL

The geometric configuration (see Figure 1(a)) is a section of a standard 2×4 residential stud wall. Starting from the inside (left), the wall consists of a 0.5-in. (0.0127-m) gypsum wallboard, a 3.5-in. (0.089-m) air cavity partially filled with fiberglass insulation, a 0.5-in. (0.0127-m) layer of sheathing, and a 1-in. (0.025-m) layer of wood siding that is exposed to outside air. Table 1 presents the material properties of different layers of the wall assembly (ASHRAE 2009). The table lists the apparent thermal conductivity for fiberglass insulation, which is based on R-15 in a 3.5-in. (0.089-m) cavity. It includes all the thermal phenomena that occur in fibrous insulation: heat conduction through the air, heat conduction through the glass, and infrared radiation exchange. The cavity is closed at top and bottom by adiabatic sills. Two cavity heights of 3-ft (found under windows) and 8-ft (full length of the wall) are considered. Simulations performed on partially filled cavities were limited to 8-ft tall cavity with insulation heights varying from 0 to 8 ft (0 to 2.44 m).

**Table 1. Properties of Building Materials Used in This Study**

| Material | Density lb/ft$^3$ (kg/m$^3$) | Conductivity Btu/h·ft·°F (W/m·K) | Specific Heat Btu/lb·°F (J/kg·K) |
|---|---|---|---|
| Gypsum wallboard | 40 (640.7) | 0.0916 (0.1584) | 0.27 (1130.4) |
| Sheathing | 18 (288.3) | 0.0316 (0.0546) | 0.31 (1297.8) |
| Wood siding | 43 (688.8) | 0.1054 (0.1823) | 0.28 (1172.3) |
| Fiberglass | 1.8 (28.8) | 0.0194 (0.0336) | 0.2 (837.3) |

All thermophysical properties—except air density, which follows the ideal gas law—are assumed to be constant and evaluated at the mean temperature for each simulation. The fiberglass insulation is modeled as a porous medium with a porosity of 0.88 and uniform air permeability. Experimental measurements for attic insulation reported by Delmas and Wilkes (1992) showed that densities varying from 0.4 lb/ft$^3$ (6.4 kg/m$^3$) to 0.9 lb/ft$^3$ (14.42 kg/m$^3$) correspond to permeabilities of $5.84 \times 10^{-8}$ and $2.7 \times 10^{-9}$ m$^2$, respectively. The fiberglass insulation used in wall cavities usually has a higher density (1.8 lb/ft$^3$ [28.8 kg/m$^3$]), for which the permeability will be much smaller[1], but since data is not available for higher densities, we used the value of $2.7 \times 10^{-9}$ m$^2$, which corresponds to the highest density available. The insulation permeability is assumed to be the same horizontally and vertically.

The fluid flow is assumed to be 2-D, laminar in the porous medium, and turbulent in the air cavity. Under steady-state conditions, the governing equations are the heat conduction equation in the structural parts of the wall and mass conservation, 2-D Navier-Stokes equations, and energy equation in the cavity. The porous medium is modeled with the addition of a momentum source term to the standard fluid flow equations. The source term is composed of a viscous loss term (Darcy) and an inertial loss term. We used the surface-to-surface method described in Modest (2003) to calculate the radiative exchange

[1] We performed a sensitivity analysis using permeability values between $10^{-9}$ and $10^{-12}$ m$^2$ and the maximum air velocity in the insulation varied from $4.17 \times 10^{-3}$ ($2.12 \times 10^{-5}$) to $1.3 \times 10^{-5}$ ft/min ($6.6 \times 10^{-8}$ m/s), which had no effect on heat transfer across the cavity or on the surface temperatures used to determine the thermal resistance.

between the inner surfaces of the wall cavity. All participating surfaces are assumed to be gray and diffuse. Surface emissivities of 0.05, 0.8, and 0.9 were considered. To examine the effect of the aspect ratio on the heat transfer through the wall, we compared a 3-ft (0.91-m) tall cavity, which can be found under windows, to the full cavity height of 8 ft (2.44 m). The model assumed a tight wall and ignored infiltration and exfiltration.

The governing equations are solved numerically using the finite volume method of FLUENT 6.3 (FLUENT Inc. 2006). Turbulence is modeled by the standard k–ε model. An implicit segregated solver is used and all discretization schemes employed are of second-order accuracy or higher. The QUICK scheme is used for momentum, energy, and density discretization. A second-order scheme is used in the pressure discretization and the SIMPLE scheme is used in pressure-velocity coupling. We assessed simulation convergence by monitoring computed conservation equations residuals and by converging surface monitors for velocity, temperature, and heat flux at select locations in the domain by setting their absolute convergence criterion to $10^{-6}$. We conducted a formal grid sensitivity study to ensure the numerical results were independent of grid resolution. We examined grid sizes ranging from 10,000 to 50,000 quadrilateral elements at the highest ΔT used (70°F [39 K]). Grid independence was within 1% with the uniform grid size of 33,304 quadrilateral elements.

## COMPARISON WITH PREVIOUS RESULTS

The numerical results obtained were compared against the results published in Chapter 26 of 2009 ASHRAE Fundamentals (ASHRAE 2009) and in Park et al. (1986). The thermal resistance of uninsulated wall cavity is compared in Tables 2 and 3. Table 2 compares the thermal resistance of a 3.5-in. (0.089-m) × 8 ft (2.44-m) cavity with that of 3.5-in. (0.089-m) air space (ASHRAE 2009) with an effective surface emissivity of 0.82. Among the five cases evaluated by Park et al. (1986), the present results are compared, in Table 3, with those of the isothermal case with pure natural convection (Case 1) and when the three heat transfer modes were combined (Case 2). Both comparisons show good agreement.

**Table 2. Comparison of Thermal Resistance of an Air Cavity***

| Mean Temperature °F (K) | Temperature Difference °F (K) | Present Work $ft^2 \cdot h \cdot °F/Btu$ ($m^2 \cdot K/W$) | ASHRAE (2009) $ft^2 \cdot h \cdot °F/Btu$ ($m^2 \cdot K/W$) | % Difference |
|---|---|---|---|---|
| 50 (283) | 30 (16.6) | 0.95 (0.17) | 0.91 (0.16) | 4.2 |
| 50 (283) | 10 (5.5) | 1.06 (0.19) | 1.01 (0.18) | 4.7 |
| 0 (255) | 20 (11.1) | 1.15 (0.20) | 1.14 (0.20) | 0.8 |
| 0 (255) | 10 (5.5) | 1.25 (0.22) | 1.23 (0.22) | 1.6 |
| -50 (228) | 20 (11.1) | 1.31 (0.23) | 1.37 (0.24) | -4.3 |
| -50 (228) | 10 (5.5) | 1.47 (0.26) | 1.50 (0.26) | -2.0 |

*Applies to a 3.5-in. (0.089-m) × 8-ft (2.44-m) air cavity against the data published in ASHRAE (2009). These results are for a surface emissivity of 0.82 and constant surface temperatures.

**Table 3. Comparison of the Thermal Resistance of a Wall Assembly***

| Case No. | Case Description | Present Work $ft^2 \cdot h \cdot °F/Btu$ ($m^2 \cdot K/W$) | Park et al. (1986) $ft^2 \cdot h \cdot °F/Btu$ ($m^2 \cdot K/W$) |
|---|---|---|---|
| 1 | Isothermal walls | 5.48 (0.97) | 5.43 (0.96) |
| 2 | Combined cond., conv., and rad. | 4.31 (0.76) | 4.31 (0.76) |

* Applies to a wall assembly containing a 3.5-in. (0.089-m) × 8-ft (2.44-m) air cavity against the results of Park et al. (1986).

## RESULTS AND DISCUSSION

Numerical simulations were performed to evaluate the thermal performance of pre-retrofit wall cavities under a wide range of ambient conditions. In all numerical results presented in this section, a constant indoor temperature of 70°F (294 K) is maintained; the outdoor ambient temperature varies from 0°F (255 K) to 120°F (322 K). The wall exchanged heat with the indoor environment at 0.68 $h \cdot ft^{2} \cdot °F/Btu$ (0.12 $m^2 \cdot K/W$) and with the outdoors at 0.17 $h \cdot ft^{2} \cdot °F/Btu$ (0.03 $m^2 \cdot K/W$). The results are presented first for the air-filled cavity without insulation and then for the partially insulated cavity. The effects of surface emissivity, ambient temperature, aspect ratio, and insulation height on temperature distribution and thermal resistance are presented and discussed. The thermal resistance values correspond to the wall cavity only, which exclude that of the structural parts of the wall.

### Uninsulated Wall Cavity

Figure 1(b) illustrates the temperature contour plots, in an 8-ft (2.44-m) tall cavity, when the ambient temperature was 30°F (272 K). The cavity dimensions in the temperature distribution plots are not to scale, to allow visualization of the flow patterns in the entire domain. Three surface emissivities (0.05, 0.8, and 0.9) are considered. At this high temperature difference between the indoors and the outdoors, a strong clockwise flow circulation was formed with high temperature gradient near the hot (left) and cold (right) vertical boundaries. Surface emissivity affected circulation intensity significantly.

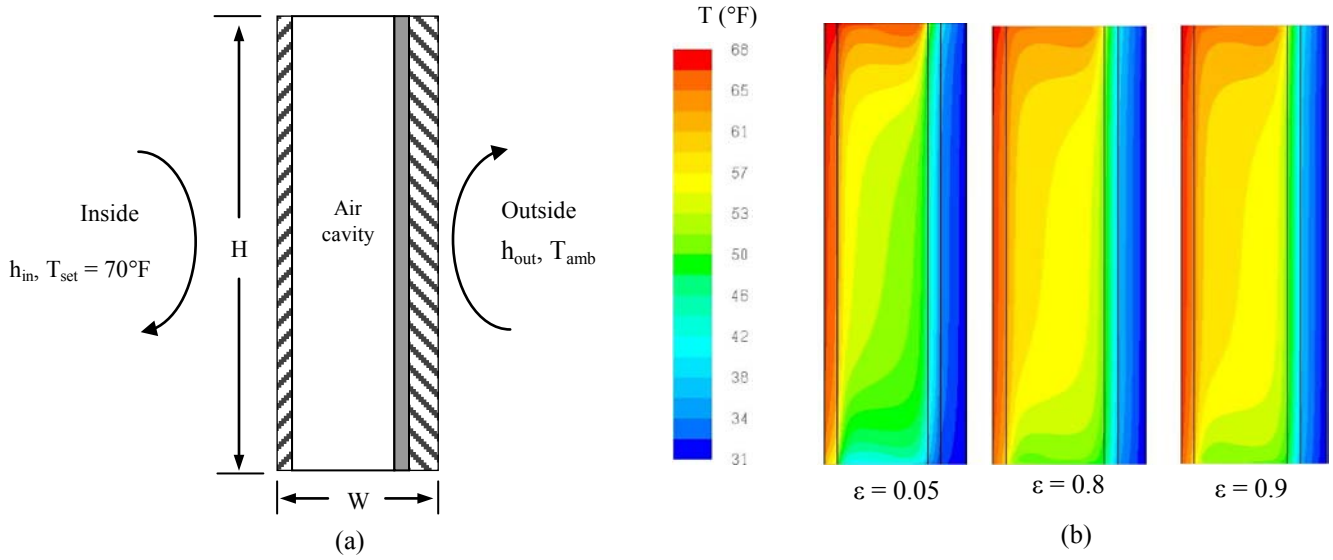


***Figure 1*** *(a) Schematic of the wall structure. (b) Effect of surface emissivity, ε, on the temperature distribution in an 8-ft (2.44-m) tall air-filled wall cavity when the outdoor ambient temperature is 30°F (272 K).*

Figure 2(a) reveals the thermal resistance, $R_C$, of the wall cavity as it varied with the ambient temperature and surface emissivity. The thermal resistance is low at 0°F (255 K) and increases with the ambient temperature to reach a maximum and then decreases at high ambient temperatures. The maximum correspondes to the condition when there is no temperature difference between the two surfaces. While the resistance of the cavity when there is no temperature difference is not very relevant, it provides an upper bound for the thermal resistance in the cavity. Near this condition, there is no air movement and while there is heat conduction through the stagnant air, thermal radiation dominates. The smaller the surface emissivity, the higher is the thermal resistance at no temperature difference.

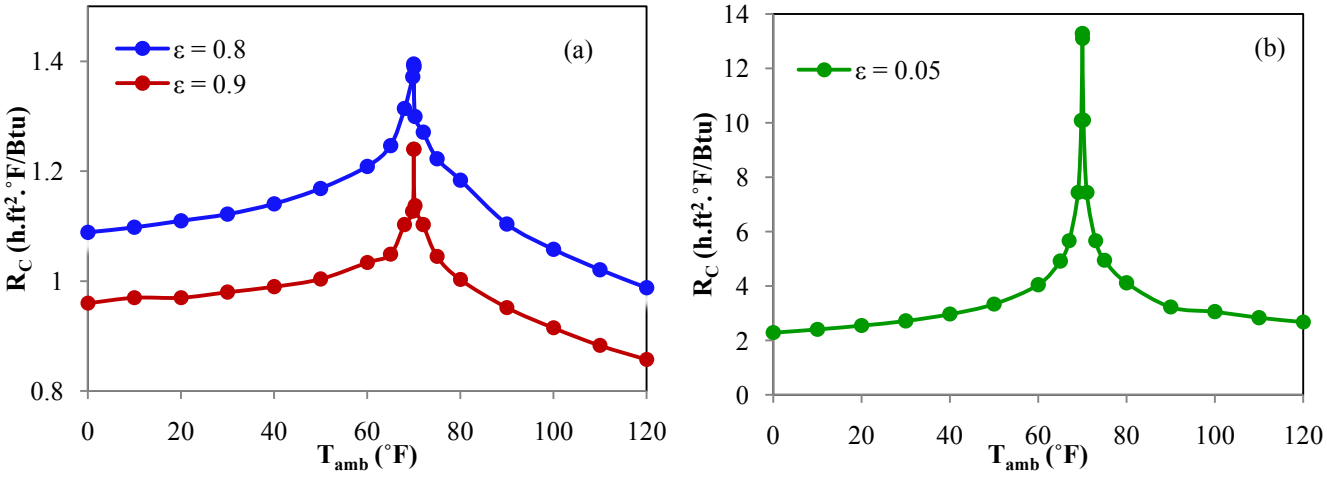


***Figure 2*** *Thermal resistance of a 3.5-in. (0.089-m) × 8-ft (2.44-m) air-filled wall cavity as a function of the outdoor ambient temperature. (a) High surface emissivities of 0.8 and 0.9 and (b) low surface emissivity of 0.05.*

Figure 3 shows the contour plots of temperature associated with ε = 0.9 and three values of ambient temperature, namely, 0°F (255 K), 30°F (272 K), and 60°F (289 K). The flow field consisted of a single circulation with high temperature gradients at low temperature (high ΔT) of 0°F (255 K). These gradients weakened as the temperature increased.

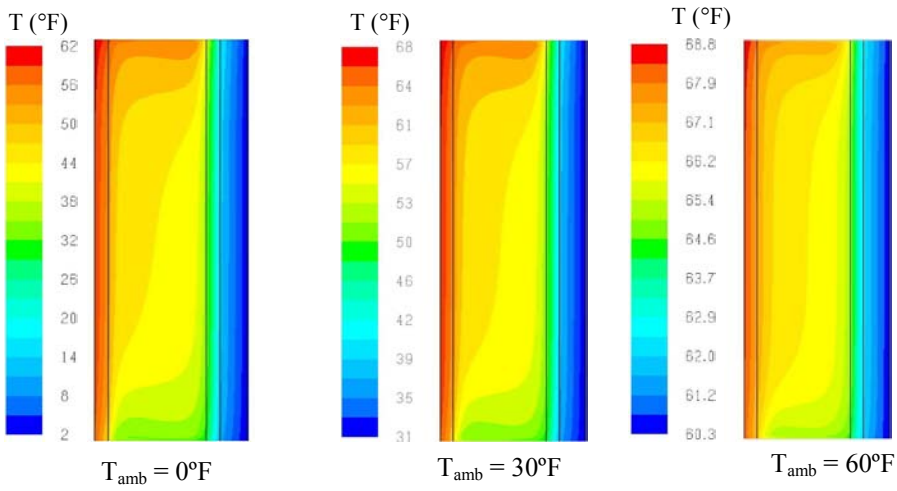


***Figure 3*** *Effect of temperature differential, ΔT, on the isotherms in an 8-ft (2.44-m) tall air-filled wall cavity when the surface emissivity is 0.9.*

To examine the thermal behavior of the wall cavity under different aspect ratios, we considered a 3-ft (0.91-m) tall cavity (found under windows) and compared the results against those from an 8-ft (2.44-m) tall cavity. Both cavities are 3.5 in. (0.089 m) wide. When the aspect ratio, A, was reduced from 27.4 (8 ft) to 10.3 (3 ft), the velocity and temperature patterns remained qualitatively the same. The only difference was in the size of the isothermal region in the cavity core. This region was larger for A = 27.4. Figure 4 shows the comparison of $R_C$ as a function of the ambient temperature and surface emissivity. $R_C$ followed the same trends shown in Figure 2. The higher aspect ratio of 27.4 presented slightly stronger resistances at ε = 0.8 and delivered stronger thermal resistance for the cavity. This difference disappeared when the emissivity was increased to 0.9.

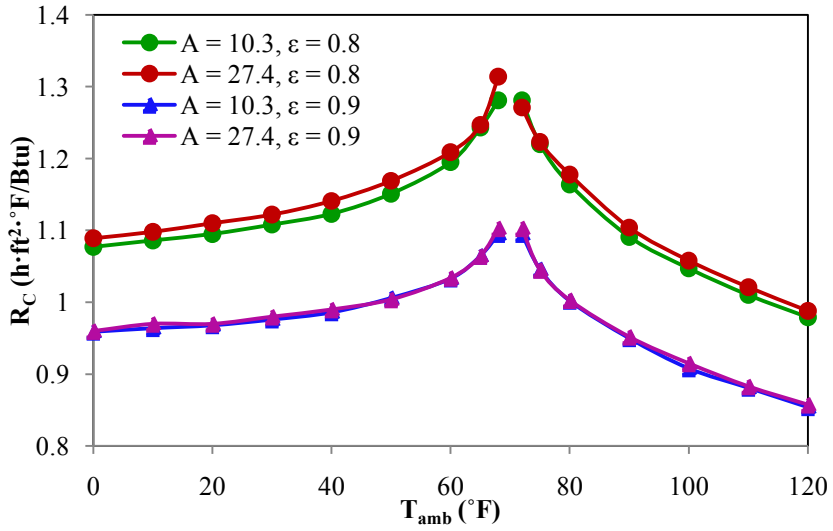


***Figure 4*** *Effect of the cavity aspect ratio, A, on the thermal resistance of a 3.5-in. (0.089-m) wide cavity filled with air. A = 10.3 corresponds to a 3-ft (0.91-m) tall cavity; A = 27.4 is for an 8-ft (2.44-m) tall cavity.*

### Partially Insulated Wall Cavity

As stated in the introduction section, partially insulated wall cavities appear in new and existing construction. Air gaps, even a few inches tall, when left uninsulated at the top of these cavities will cause significant reduction in the thermal resistance of the wall. This section discusses the impact of thermal shorts caused by these air gaps on the overall thermal resistance of the wall cavity.

Figure 5 illustrates the temperature distribution in the upper region of the wall, which has an air gap above the insulation. The corresponding heat flux profiles along the warmer inner surface of the wall exchanging heat with the room air are presented in Figure 6. Three insulation heights with a 4-in. (0.1 m), a 1-ft (0.3 m), and a 2-ft (0.61 m) tall air gaps are presented from left to right. At this ambient temperature of 30°F (272 K), there is a strong air circulation in the uninsulated part of the cavity with higher temperature gradient in the smallest air cavity. The isotherms in the insulation are straight over the entire length of the insulation, except in the region between the insulation and the air gap where the isotherms are deformed by the heat exchange caused by the air circulation in the uninsulated part. The 1-D temperature profiles indicate that heat transfer across the insulated domain does not experience convection. Each curve of Figure 6 illustrates the distribution of the local heat flux at a typical insulation height. The heat flux dominated by diffusion at the bottom of the wall remains uniform up to the interface of the insulation and the air gap. Over the air gap height, at the upper region, the heat flux increased quickly to reach a maximum at the bottom of the air gap and decreased again near the top. The high heat flux in the air gap is attributed to radiation and natural convection.

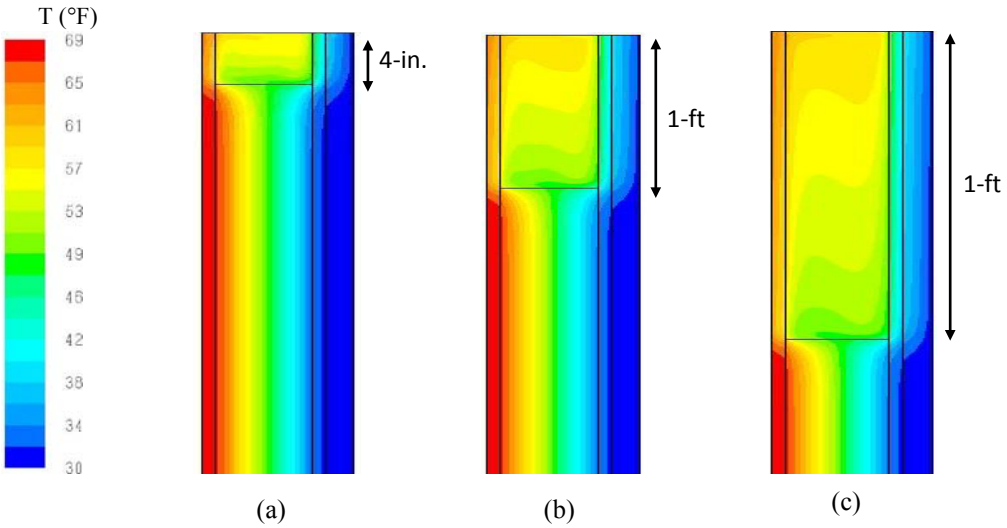


***Figure 5*** *Temperature distribution in the upper section of an 8-ft (2.44-m) tall partially insulated wall cavity. (a) 4-in tall air gap, (b) 1-ft tall air gap, and (c) 2-ft tall air gap. These results are for 0.9 surface emissivity and 30°F (272 K) ambient temperature.*

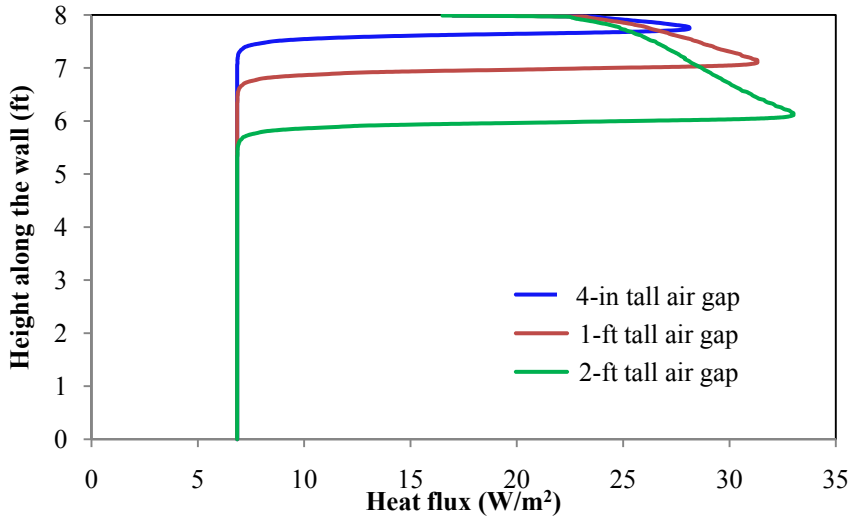


***Figure 6*** *Heat flux along the inner surface of the wall exchanging heat with the room air. These results for an 8-ft (2.44-m) tall partially filled wall cavity when the surface emissivity is 0.9 and 30°F (272 K) ambient temperature.*

Figure 7 shows the cavity thermal resistance as a function of the ambient temperature and insulation height. Each curve represents one insulation level and the figure covers different insulation levels from an uninsulated cavity to a fully insulated cavity. Regarding the upper curve representative of the fully insulated cavity, which constitutes a base case for comparison, $R_C$ is constant and equal 15 h·ft²·°F/Btu (2.64 m²·K/W). With a 3.8-in. (0.089 m) tall air gap, the thermal resistance drops by 15%. Similarly, a 1-ft tall air gap led to a 35% decrease and a 2-ft tall air gap led to a 54% decrease in thermal resistance.

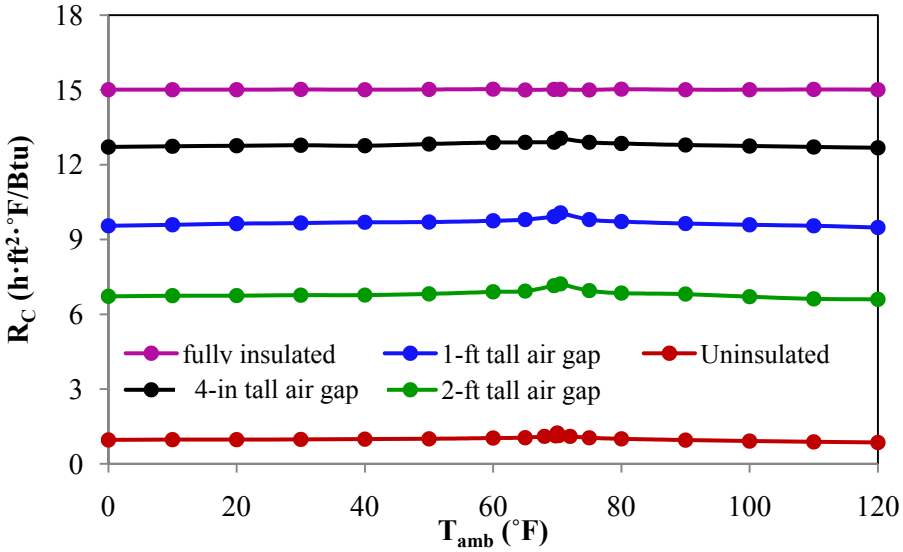


***Figure 7*** *Thermal resistance of a partially insulated wall cavity as a function of insulation height and ambient temperature. These results are for a 3.5-in. (0.089-m)× 8-ft (2.44-m) cavity with 0.9 surface emissivity.*

Figure 8 compares the thermal performance of the wall assembly, with temperature dependent $R_C$, against the results of constant $R_C$ when the surface emissivity is 0.8. The comparison was done in terms of the total heat flux through the wall assembly for the two limiting cases of uninsulated and fully insulated wall cavities. For the temperature independent case, we used the value of $R_C$ corresponding to an average temperature of 75°F and a temperature difference, ΔT, of 50°F. The heat flux increases almost linearly with ΔT. Differences between the two approaches are up to 6% for $|\Delta T|$ greater than 10°F. The larger variations at very low temperature differences that can be seen in the figure are not significant because of the small heat transfer rates at low temperature differences. While both radiation and convection heat fluxes through the uninsulated

cavity depend on the temperature, the resistance of the uninsulated cavity is small compared to the air films and the other layers in the wall assembly, which makes the effect on the overall heat flux small. The fully insulated case is also shown in Figure 8 for comparison.

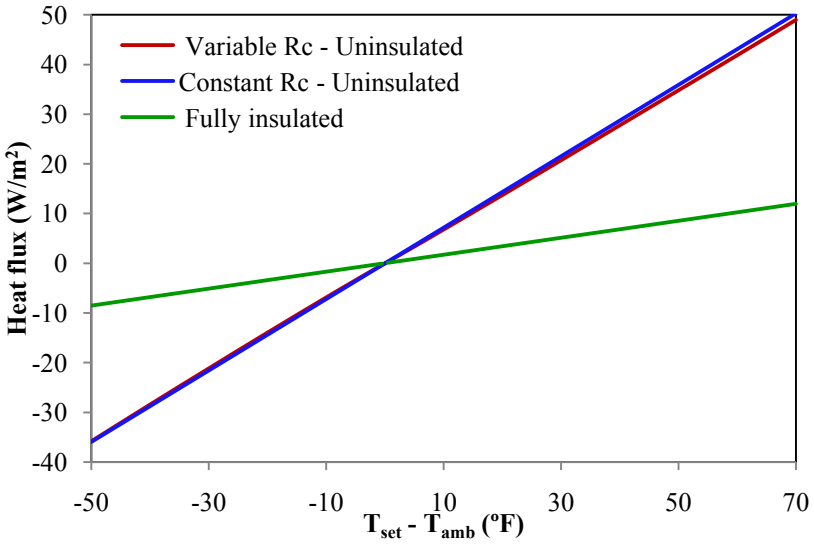


***Figure 8*** *Total heat flux through a wall assembly containing an 8-ft (2.44-m) tall cavity as a function of temperature difference between the indoor and the outdoors when the surface emissivity is 0.8.*

Figure 9 shows the total thermal resistance, $R_{tot}$, of the wall assembly including the cavity, wallboard, sheathing, wood siding, and the inside and the outside film resistances. This resistance was evaluated as a function of insulation height in an 8-ft (2.44-m) tall cavity at 30°F (272 K) ambient temperature. Also presented in this figure are the results from the approach based on two parallel resistances: one through the insulation and one through the air gap. We used the ASHRAE (2009) data for the resistance of the air gap. As the insulation height increases, the thermal resistance increases. When comparing the two approaches, the results are almost identical with a maximum difference of 3%. This difference occurred for the uninsulated limiting case.

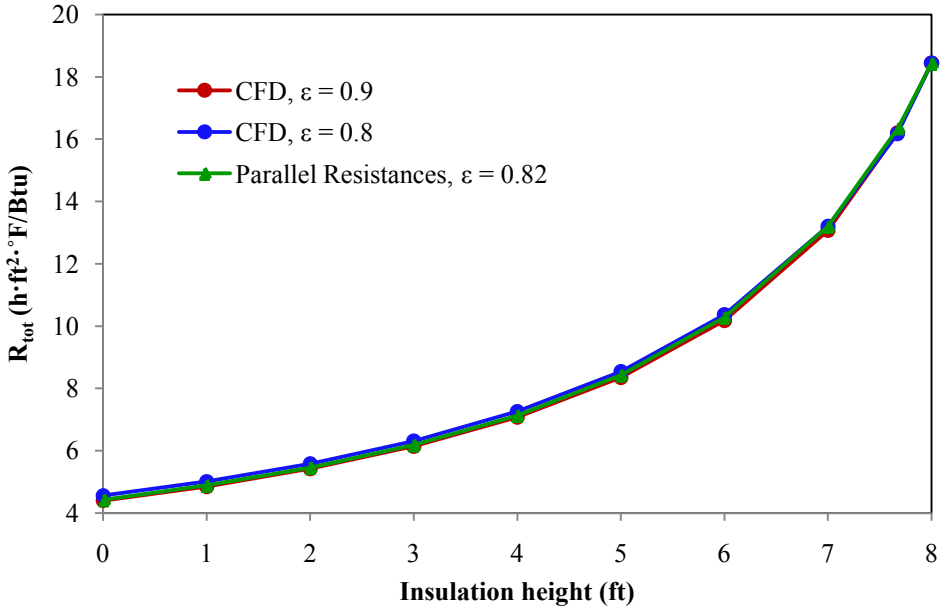


***Figure 9*** *Evolution of thermal resistance with insulation height with 30°F (272 K) ambient outdoor temperature.*

## CONCLUSIONS

Numerical simulations were performed to evaluate the thermal performance of wall cavities, presented by temperature distribution, local heat flux along the wall, and thermal resistance of the wall cavity for different temperature differences and average temperatures. Parameters were ambient outdoor temperature, cavity surface emissivity, cavity aspect ratio, and insulation height. A detailed study of the thermal performance of partially (vertically) insulated wall cavities is revealed by presenting the evolution of the thermal resistance, with insulation height, in a 3.5-in. (0.089-m) × 8-ft (2.44-m) wall cavity.

The followings are the key findings of this study:

- As expected, for a partially filled cavity, a small air gap can lead to a significant reduction in resistance. For instance, a 4-in. tall (0.1-m) air gap led to a 15% reduction in resistance. Similarly, a 2-ft (0.6-m) tall air gap led to 54% reduction in thermal resistance.
- While the thermal resistance of an uninsulated cavity varies with temperature, since it is small when compared to the resistance of the other layers and of the external and internal air films, the difference in heat flux through the wall assembly does not vary much with temperatures. The difference in the total heat flux between constant and variable cavity resistances varied between 2% and 6% when the temperature difference is greater 10˚F.
- The parallel resistance approach predicts well the resistance of wall assemblies with partially filled wall cavities, with maximum error of 3%.

## REFERENCES


Abourida, B., Hasnaoui, M., and Douamna, S. 1999. Transient Natural Convection in a Square Enclosure with Horizontal Walls Submitted to Periodic Temperatures, Numerical Heat Transfer A 36: 373–750.

Akiyama, M., and Chong, Q.P. 1997. Numerical Analysis of Natural Convection with Surface Radiation in a Square Enclosure. Num. Heat Transfer A 31: 419–433.

Antar, M.A., and Baig, H. 2009. Conjugate Conduction-Natural Convection Heat Transfer in a Hollow Building Block. Applied Thermal Engineering 29(17-18): 3716–3720.

ASHRAE. 2009. ASHRAE Fundamentals Handbook. Atlanta: American Society of Heating Refrigeration and Air-Conditioning Engineers, Inc.

Aviram, D.P., Fried, A.N., and Roberts, J.J. 2001. Thermal Properties of a Variable Cavity Wall. Building and Environment 36(9): 1057–1072.

Catton, I. 1978. Natural Convection in Enclosures. Proceeding of the Sixth Int. Heat Transfer Conference 6: 13–32.

Delmas, A.A., and Wilkes, K.E. 1992. Numerical Analysis of Heat Transfer by Conduction and Natural Convection in Loose-Fill Fiberglass Insulation – Effects of Convection on Thermal Performance, ORNL Technical Report, CON-338, Oak Ridge National Laboratory.

Douamna, S., Hasnaoui, M., and Abourida, B. 2000. Two-Dimensional Transient Natural Convection in a Repetitive Geometry Submitted to Variable Heating from Below: Numerical Identification of Routes Leading to Chaos. Numerical Heat Transfer A 37: 779–799.

FLUENT Inc. 2006. FLUENT Manual. Lebanon, NH, FLUENT, Inc.

Fusegi, T., Hyun, J.M., Kuwahara, K. 1992. Natural Convection in a Differentially Heated Square Cavity with Internal Heat Generation, Numerical Heat Transfer A 21: 215–229.

Jaluria, Y. 2003. Natural Convection, in Heat Transfer Handbook, chap. 7, A. Bejan and A. D. Kraus (eds.), Wiley, New York.

Barbour, E., Goodrow, J., Kosny, J., Christian, J. E. 1994. Thermal Performance of Steel-Framed Walls. CRADA Final Report for ORNL93-0235

Lakhal, E.K., Hasnaoui, M.,; Vasseur, P., and Bilgen, E. 1995. Natural Convection in a Square Enclosure Heated Periodically from Part of the Bottom Wall. Numerical Heat Transfer A 27: 319–333.

Lorente, S. 2002. Heat Losses through Building Walls with Closed, Open and Deformable Cavities. International Journal of Energy Research 26(7): 611-632.

Manz, H. 2003. Numerical Simulation of Heat Transfer by Natural Convection in Cavities of Facade Elements. Energy and Buildings 35(3): 305-311.

Modest, M.F. 2003. Radiative Heat Transfer, 2nd ed., Academic Press, CA.

Pak, H.Y., and Park, K.W. 1998. Numerical Analysis of Natural Convective and Radiative Heat Transfer in an Arbitrarily Shaped Enclosure, Numerical Heat Transfer A 34: 553–569.

Park, J.E., Kirkpatrick, J.R., et al. 1986. Calculation of Heat Flux through a wall Containing a Cavity: Comparison of Several Models. Oak Ridge Gaseous Diffusion Plant, TN, DE86010348.

Rahman M., and Sharif, M.A.R. 2003. Numerical Study of Laminar Natural Convection in Inclined Rectangular Enclosures of Various Aspect Ratios. Numerical Heat Transfer A 44: 355–373.

Raithby, G.D., and Hollands, K.G.T. 1998. Natural Convection In Handbook of Heat Transfer, W. M. Rohsenow et al. (eds.), 3d ed., McGraw-Hill, New York.

Vafai, K., and Belwafa, J. 1990. An Experimental Investigation of Heat Transfer in Enclosures Filled or Partially Filled With a Fibrous Insulation. ASME Journal of Heat Transfer 112: 793–797.

Xaman, J., Alvarez, G., Lira, L., and Estrada, C. 2005. Numerical Study of Heat Transfer by Laminar and Turbulent Natural Convection in Tall Cavities of Facade Elements. Energy and Buildings 37(7): 787–794.

Yang, K.T. 1987. Natural Convection in Enclosures, in Handbook of Single-Phase Heat Transfer, S. Kakac et al. (eds.), Wiley, New York.

Yucel, A., Acharya, S., and Williams, M.L. 1989. Natural Convection and Radiation in a Square Enclosure, Numerical Heat Transfer A 15: 261–278.